*Progress In Electromagnetics Research, Vol. 148, 41–53, 2014*

# Novel Short Tapered Leaky Wave Antennas with Complementary Split Ring Resonator for Back Lobe Suppression

**Jie-Huang Huang*, Chien-Rung Huang, and Christina F. Jou**

**Abstract**—Two novel short tapered leaky wave antenna (LWA) designs with a complementary split ring resonator (CSRR) structure are proposed in this paper. The CSRR structure is positioned at $1/4\lambda_g$ away from the open-end edge of the LWA. For one of the antenna designs, the CSRR is placed at the ground plane; for the other one, the CSRR is placed on the antenna plane. The reflected wave caused by the open-end edge of the LWA is cancelled by the reflected wave caused by the CSRR, thus, the back lobe can be effectively suppressed. The length of these two short tapered LWAs with CSRR design is only $1.2\lambda_g$ at 4.3 GHz. According to the measurement results, the impedance bandwidth is 650 MHz for 7 dB return loss, which covers the range from 4.3 GHz to 4.95 GHz. The back lobe can be suppressed effectively about more than 12 dB at the whole operating frequency band. The scanning range of the main beam is about 34°, which cover the scanning angle from 10° to 44°.

## 1. INTRODUCTION

Leaky wave antennas (LWAs) have been studied for past several years. The first LWA prototype was presented by Menzel in 1978 [1], which used an asymmetric feed line to excite the first higher order mode. Subsequently, Oliner and Lee proposed the complex propagation constant theory of the leaky mode in 1986 [2]. LWA has attracted considerable interest since its characteristics of narrow beamwidth, wideband bandwidth, frequency-scanning capability and fabrication simplicity [3]. Because of these advantages, LWAs are usually adopted in the satellite communication or scanning systems such as traffic control and collision avoidance system.

Despite owning many advantages, the LWA still faces a major problem which is the trade-off between the back lobe and the length of the LWA. As well known, to obtain low back lobe and effective radiation, the length of an LWA is required about $4 \sim 5\lambda_0$, which occupies considerable large size. Therefore, the length of an LWA is often reduced to shorter than $2\lambda_0$ for the size consideration. However, the induced back lobes will be increased if the antenna length is shortened since most of the non-radiated power (or non-leaked power) is reflected at the open-end edge of the LWA.

For the back lobe suppression consideration of short length LWAs, several researches have been proposed with different approaches in recent years. One of the approaches reuse the non-radiated power to suppress the reflected power which causes the back lobe [4–6]. This method can suppress the back lobe more than 10 dB; however, this method makes the antenna design become more complicated. Another approach to suppress the back lobe is disturbing the current distribution at the open-end edge of the LWA to reduce the backward reflected power and guiding the non-radiated power to ground plane [7]. This approach improved the back lobe level better than 10 dB at lower operating frequency, but the back lobe was suppressed about only 6 dB in higher operating frequency band. For another approach to improve the back lobe level, several studies are using tapered structure [8–10]. This method also modifies the current distribution by the sections with different widths. Moreover, the slot structure is

*Received 26 February 2014, Accepted 9 May 2014, Scheduled 1 July 2014*

* Corresponding author: Jie-Huang Huang (double0303@gmail.com).

The authors are with the Institute of Communications Engineering, National Chiau-Tung University, 1001 University Road, Hsinchu, Hsinchu, Taiwan, R.O.C.

used to improve the back lobe level in [8, 9]. However, the back lobe at higher operating frequency range is still an issue, and the side lobe at lower half plane is induced simultaneously. Here, in this paper, the complementary split ring resonator (CSRR) structure is adopted to modify the current distribution of the LWA at higher operating frequency.

Recently, the CSRR structure has attracted great interest in the microwave circuit and antenna designs. Demonstrating the characteristic in [11], the CSRR is the dual counterpart of the split ring resonator (SRR) which is first proposed by Pendry et al. [12]. The CSRR structure provides a negative effective permittivity to the structure, which is used to be left-handed (LH) metamaterials. Besides, the signal propagation is precluded in the CSRR structure when operating at the resonant frequency. Due to these characteristics, some research using the CSRR structure to implement the composite right/left handed (CRLH) structure [13]. For the resonance characteristic of the CSRR structure, there are several applications in band-pass filter [14–16] and low-pass filter design [17]. Another application for antenna design is using CSRR structure to reject unwanted frequency band in wide bandwidth antenna design [18]. Moreover, the CSRR structure is also used in other antenna designs to achieve size miniaturization [19–21].

In this paper, two designs for back lobe suppression are demonstrated. Both of them are short tapered leaky wave antennas embedded with the CSRR structure. The difference between the two designs is the location of the CSRR. This design method can suppress the back lobe of the LWA effectively. The back lobe level can be better than 12 dB at the whole operating frequency band. The design procedure of the proposed antennas is discussed in Section 2. The parameters discussion and comparison results are also demonstrated in this section. The measurement results are illustrated in Section 3. Finally, the conclusion is given in Section 4.

## 2. ANTENNA DESIGN

The concepts of the proposed antennas are discussed in this section which is divided into three subsections. First, the conventional LWA will be briefly introduced, and the tapering structure is utilized to improve the performance of the LWAs. Next, the second subsection proposes the CSRR structure which is the most significant design method of this paper. The last subsection demonstrates the proposed LWAs with parameters discussion.

### 2.1. The Conventional Leaky Wave Antenna

For conventional LWAs, the normalized propagation constant $\beta/k_0 - j\alpha/k_0$ controls the radiation region (which is also called leaky mode region) bandwidth and the radiation pattern. The normalized propagation constant includes normalized phase constant $\beta/k_0$ and normalized attenuation constant $\alpha/k_0$, where $k_0$ is the free space wavenumber. Both of the constants are a function of frequency, as shown in Fig. 1(a). The function can be obtained by using a rigorous (Wiener-Hopf) solution [22, 23]. The solution is determined by width of the LWA, dielectric constant and substrate thickness. A FR4 substrate is used in this study with thickness $H = 0.8\,\text{mm}$, relative dielectric constant $\epsilon_r = 4.3$, $\tan\delta = 0.02$, and width of the LWA $W = 16\,\text{mm}$.

The leaky mode region starts from the frequency while $\beta/k_0$ is equal to $\alpha/k_0$ and stops at the frequency when the $\beta$ is equal to the free-space wavenumber $k_0$. According to Fig. 1(a), the leaky mode region is from 4.3 GHz to 4.9 GHz. In this region, the traveling wave starts to leak power into air, which is also seen as radiation. Moreover, the radiation pattern parameters such as the angle of mainbeam $\theta_m$ and radiation 3-dB beamwidth $\Delta\theta$ have relationship with the normalized phase constant and normalized attenuation constant, respectively. $\theta_m$ and $\Delta\theta$ can be approximated as following:

$$\sin\theta_m \simeq \frac{\beta}{k_0} \tag{1}$$

$$\frac{\alpha}{k_0} \simeq 0.183 \times \Delta\theta \times \cos\theta_m \tag{2}$$

$$\frac{L}{\lambda_0} \simeq \frac{0.183}{\alpha/k_0} \tag{3}$$

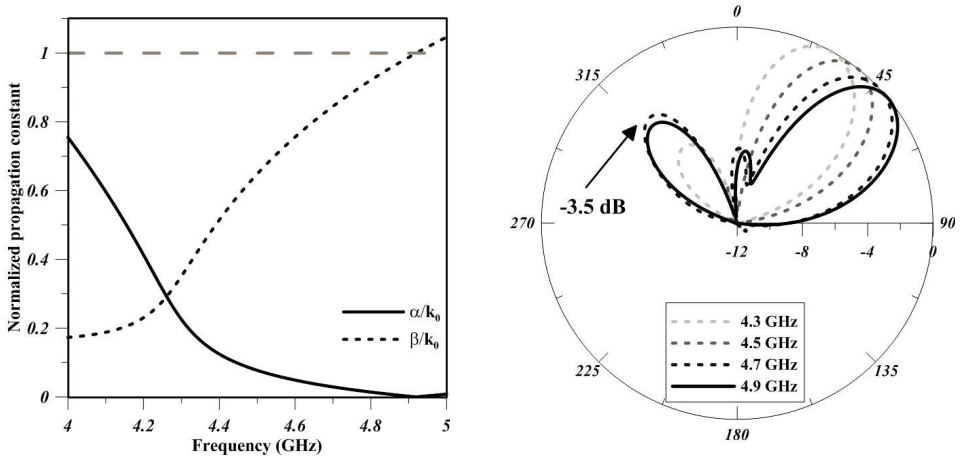


**Figure 1.** Characteristics of the conventional microstrip LWA in which $H = 0.8\,\text{mm}$, $\epsilon_r = 4.3$, $\tan\delta = 0.02$, and $W = 16\,\text{mm}$. (a) Normalized complex propagation constant. (b) Simulated radiation pattern result.

where $L$ is the length of the LWA and $\lambda_0$ the free space wavelength of the operating frequency. Based on (3), the length of the LWA can be determined when 90% of the radiated power is achieved. Although the scanning angle $\theta_m$ is a function with the phase constant $\beta$ and wavenumber of free space $k_0$, the length of LWA also has relationship with the angle. Table 1 lists the simulated results of the scanning angle $\theta_m$ with different antenna lengths while the LWA operating at 4.9 GHz. Refering to Table 1, the maximum scanning angle becomes smaller while the antenna length is shorter.

**Table 1.** Scanning angle $\theta_m$ at 4.9 GHz.

| Antenna Length | $1\lambda_0$ | $1.2\lambda_0$ | $1.5\lambda_0$ | $2\lambda_0$ | $3\lambda_0$ | $4\lambda_0$ |
|---|---|---|---|---|---|---|
| Maximum $\theta_m$ | 45° | 52° | 55° | 57° | 64° | 67° |

In this study, for the antenna size consideration, we implement the short length LWA. However, the back lobe level becomes worse since the length of the antenna is too short that most of the input wave is unable to leak to air. Then, the non-leaked wave is reflected at the LWA edge, which causes the back lobe. Fig. 1(b) shows the simulated radiation pattern results of the conventional short LWA of which the length is 84 mm ($1.2\lambda_0$ at 4.3 GHz), and the width is 16 mm. Compared with the main lobe, the back lobe is quite large.

To suppress the back lobe, this work firstly utilizes the tapering structure which is one of the most well-known approaches [8–10]. Since the tapering method increases the normalized attenuation constant and reshapes the current distribution, the back lobe can obtain effective suppression while the LWA is operating in leaky mode. As the simulation results shown in Fig. 2, the tapering method improves the back lobe level. For lower frequency band (4.3 GHz $\sim$ 4.6 GHz), the back lobe has been suppressed better than 12 dB. However, the back lobe of higher operating frequency (4.7 GHz $\sim$ 4.9 GHz) still requires more suppression. Meanwhile, the scanning angle tilts toward broadside since the tapering method reduces width of the LWA and results in the phase constant decreasing in the leaky mode region. Therefore, to suppress the back lobe for higher operating frequency and maintain the original leaky mode region, this study makes the CSRR structure embedded in short tapered LWA for back lobe level improvement.

### 2.2. Complementary Split Ring Resonators

Complementary split ring resonator, the dual counterpart of the split ring resonator, is one of the electromagnetic metamaterials structure which is broadly called left-handed structure [24]. It generates

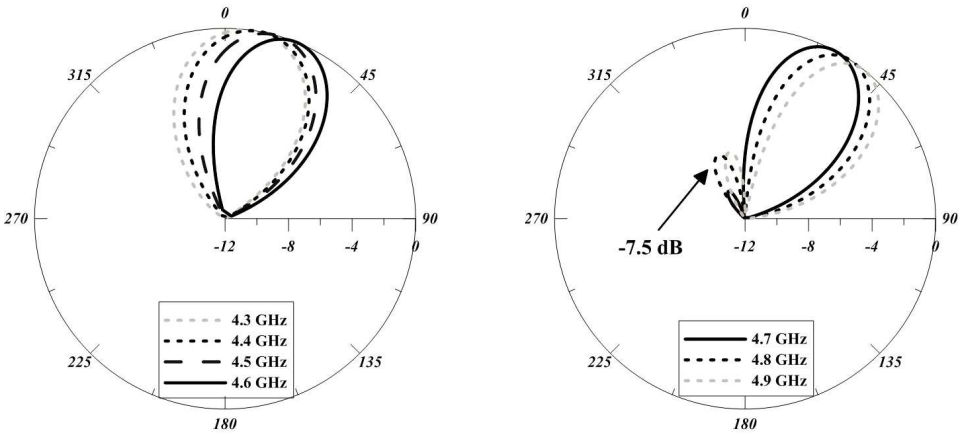


(a) Lower frequency band (b) Higher frequency band

**Figure 2.** Simulated radiation pattern of the tapered LWA.

a significant phenomenon which is called stop band. This characteristic can suppress the wave propagation. To be detailed, the CSRR structure has the resonance characteristic, which can be modeled as a resonator circuit composed of a capacitor and an inductor as shown in Fig. 3, where $R_0$ is the mean radius of the CSRR, $d$ the width of the CSRR, and $g$ the gap width.

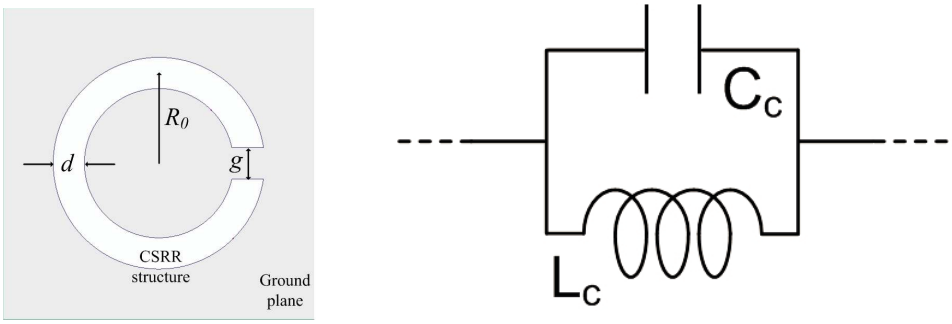


(a) (b)

**Figure 3.** Equivalent lump circuit of single CSRR structure. (a) Single CSRR structure. (b) Equivalent lumped element circuit.

The resonance frequency of a single CSRR can be approximately obtained since the perimeter of the single CSRR matches a half guided wavelength as shown in following:

$$L_r = 2\pi R_0 - g \approx \frac{1}{2}\lambda_g \tag{4}$$

where $\lambda_g$ is the guided wavelength. Since the resonance frequency is related to the perimeter, $L_r$, the dimension of the CSRR can be determined. Moreover, the equivalent lump circuit for a microstrip line with a pair CSRR structure is shown in Fig. 4. The design parameters are the same as shown those in Fig. 3(a). The new introduced parameter, $s$, is the spacing between the two CSRR.

Figure 5(a) displays the simulated insertion loss with different gap values, and $L_r$ is fixed to 14.7 mm, or about $1/2\lambda_g$ of 4.9 GHz. Based on the result, the resonance frequency depends on the value of gap. Since the gap value is related to the capacitance and inductance of the equivalent circuit of the CSRR structure, although $L_r$ is fixed, the resonance frequency is changed with different gap values. According to Fig. 5(a), the resonance frequency is varied from 4.5 GHz to 5 GHz as the gap is varied from 1.5 mm to 0.5 mm. However, the other parameter of the single CSRR, $d$, has slight effect on the resonance frequency. Fig. 5(b) shows the simulated results with different widths, $d$. The different

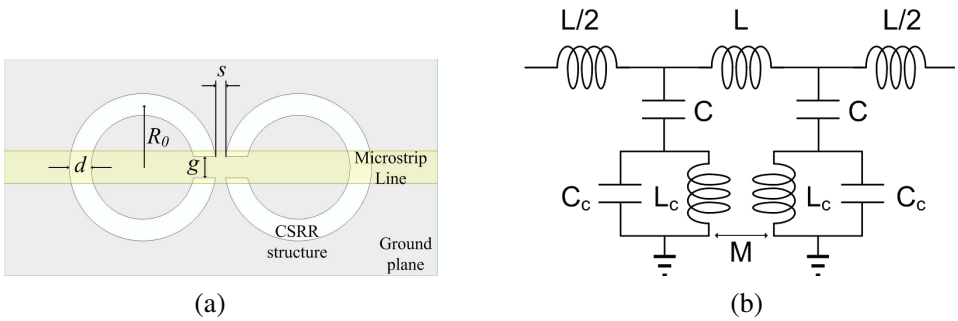


**Figure 4.** Equivalent lump circuit of a pair of single CSRR loaded microstrip line. (a) A pair of single CSRR structure loaded microstrip line. (b) Equivalent lump circuit.

width cases have insignificant effect on resonance frequency since the width, $d$, is independent of the resonance frequency of the CSRR structure. As mentioned in (4), the resonance frequency is unrelated with width, $d$. For the other parameter of the whole CSRR structure, the spacing, $s$, it is related to the mutual inductance between the two CSRRs. Referring to the equivalent lump circuit shown in Fig. 4, the mutual inductance, $M$, is related to the resonance frequency of the whole CSRR structure. Fig. 5(c) shows the simulated insertion loss with different spacings. Here, the perimeter, $L_r$, is still fixed at 14.7 mm. According to the results, the resonance frequency shifts to higher frequency while the spacing is increased. Because the spacing is inversely proportional to the mutual coupling effect, the coupling factor and mutual inductance are also inversely proportional to the spacing. Therefore, the resonance frequency of the whole CSRR structure is also inversely proportional to the spacing.

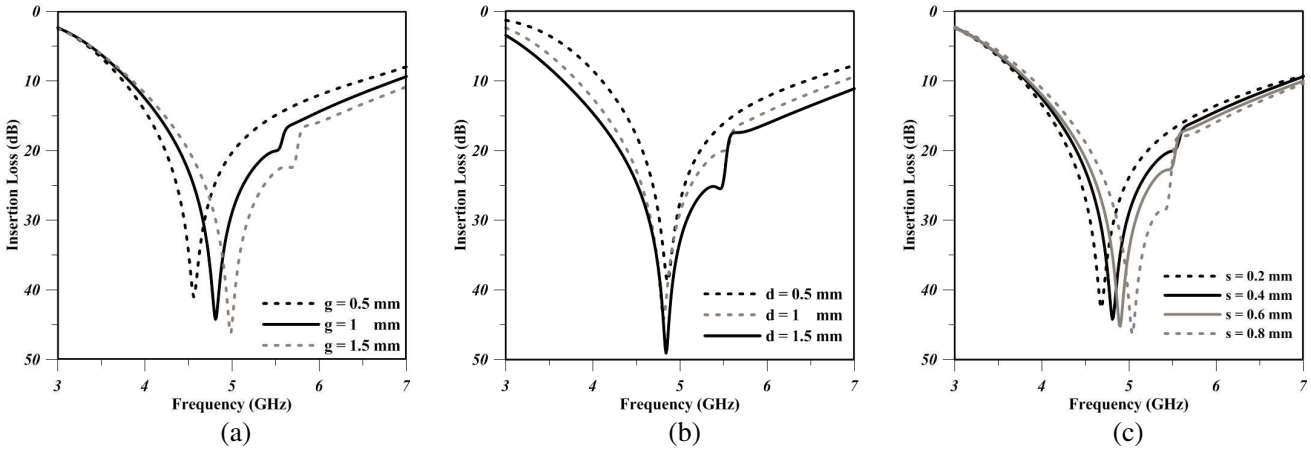


**Figure 5.** The insertion loss of the 50 Ω transmission line with a pair of CSRR structure and the perimeter $L_r$ is fixed to be 14.7 mm. (a) With different gap case. (b) With different width case. (c) With different spacing case.

### 2.3. Short Tapered Leaky Wave Antenna Design with Complementary Split Ring Resonator

The configurations of the two proposed LWAs are shown in Fig. 6. The two antennas are short tapered LWAs embedded with CSRR structure. Both of them are printed on a 0.8-mm-thick FR-4 substrate. The dielectric constant ($\epsilon_r$) and loss tangent ($\tan\delta$) are 4.3 and 0.02, respectively. The difference between these two designs is the position of the CSRR structure. For the first design, the CSRR structure is located at the ground plane as shown in Fig. 6(a). The other is similar to the first design except the position of the CSRR structure which is on the antenna structure plane, as shown in Fig. 6(b). The

length of both proposed LWAs is 84 mm, which is about $1.2\lambda_0$ at 4.3 GHz. The antenna width is tapered from 16 mm ($W_1$) to 13.5 mm ($W_2$) in order to improve back lobe level at lower frequency band. The other design parameters are listed in Table 2.

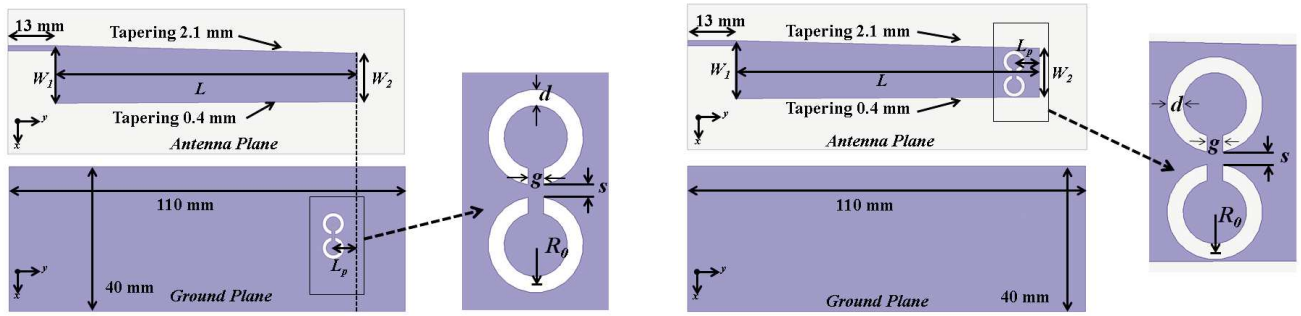


**Figure 6.** Structure of the proposed antennas. (a) Short tapered LWA with CSRR structure at ground plane. (b) Short tapered LWA with CSRR structure on antenna plane.

**Table 2.** Dimensions of the proposed LWA (Unit: mm).

| Parameters | $L$ | $R_0$ | $s$ | $g$ | $W_1$ | $W_2$ | $d$ | $L_p$ |
|---|---|---|---|---|---|---|---|---|
| Dimension | 84 | 2.5 | 0.4 | 1 | 16 | 13.5 | 1 | 7 |

In this study, the dimension of the CSRR is determined by the resonance frequency which is chosen to be around the higher operating frequency of the LWA to suppress the back lobe of the higher frequency band. Therefore, the average radius of the split ring, $R_0$, is chosen to be 2.5 mm; width of the split ring, $d$, is 1 mm; the gap of the split ring, $g$, is 1 mm. The perimeter of the split ring ($L_r$) is about 14.7 mm, which is about $\lambda_g/2$ of 4.9 GHz to suppress the back lobe at higher operating frequency.

The current distribution of the short tapered LWAs with and without CSRR structure simulation results comparison are demonstrating in Fig. 7 that all of the antennas are operating at 4.9 GHz. According to the results, the current is concentrated at the CSRR structure so that the backward wave which causes the back lobe can be decreased effectively.

For the design parameters, the mean radius, $R_0$ and gap, $g$, of the CSRR structure dominate the resonance frequency as mentioned in (4). These two parameters are closely correlated with the equivalent inductor and capacitor as shown in Fig. 3. Fig. 8 displays the simulated radiation pattern results with different gap cases in which the perimeter, $L_r$, is fixed at 14.7 mm. According to the results, the gap is chosen to be 1 mm in this study to obtain effective back lobe suppression which is better than 12 dB. For the other different gap cases, the back lobes are worse than 10 dB. Although the perimeter has been fixed, the back lobe is still influenced. Since the current distribution is highly interfered by the CSRR geometry, the gap of the CSRR is one of the important factors that can improve the back lobe level.


**Figure 7.** The comparison current distribution operating at 4.9 GHz of proposed short taper LWA without and with a pair of single CSRR structure. (a) Without the CSRR structure. (b) With the CSRR structure at ground plane. (c) With the CSRR structure on antenna plane.

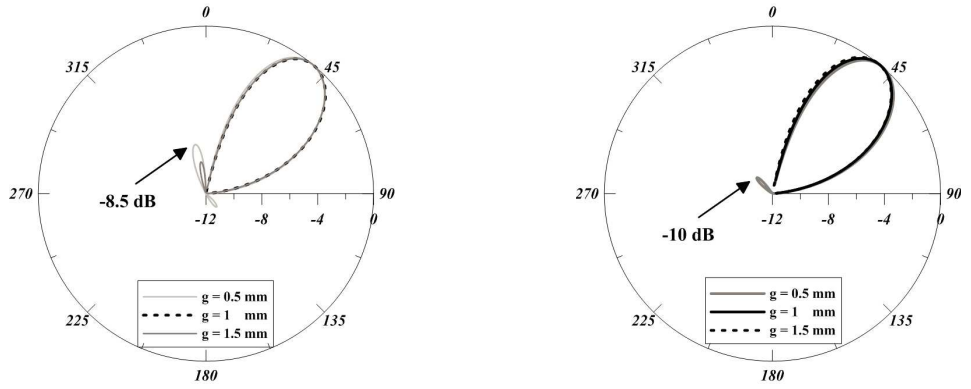


(a) (b)

**Figure 8.** Simulated radiation patterns at 4.9 GHz with different gap, $g$, where the perimeter $L_r$ is fixed to be 14.7 mm, CSRR width $d$ is fixed to be 1 mm and spacing $s$ is fixed to be 0.4 mm. (a) CSRR at ground plane. (b) CSRR on antenna plane.

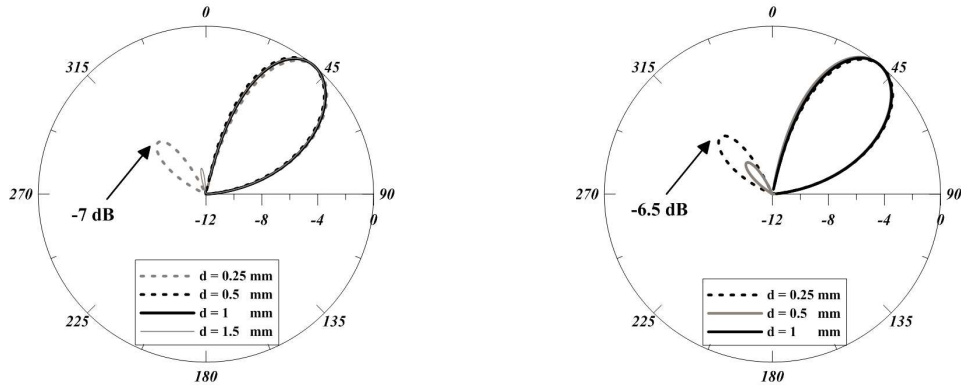


(a) (b)

**Figure 9.** Simulated radiation patterns at 4.9 GHz with different width, $d$, where the perimeter $L_r$ is fixed to be 14.7 mm, the gap $g$ is fixed to be 1 mm and spacing $s$ is fixed to be 0.4 mm. (a) CSRR at ground plane. (b) CSRR on antenna plane.

As shown in (4), the width, $d$, of the CSRR structure has no relationship with the resonance frequency, as shown in Fig. 5(b). However, the width, $d$, of the CSRR structure has effect on the back lobe suppression. Fig. 9 displays the simulated radiation pattern results with different widths for both cases. Since the current distribution has been disturbed by adding the CSRR structure, the width of the CSRR is related to the current distribution. The influence of the narrow width is rather slight, so the back lobe is still quite large; however, the wider width decreases the back lobe suppression. According to the results, the back lobe can be suppressed effectively, better than 12 dB at $d = 1$ mm.

The spacing, $s$, between the two single CSRR structures is another design parameter in this study. The two single CSRR structures have coupling effect with each other; therefore, the mutual coupling factor depends on the spacing of these two CSRRs. According to Fig. 5(c), the resonance frequency is about 4.8 GHz while the spacing is 0.4 mm. Since the spacing affects the resonance frequency of the whole CSRR structure, the value of the spacing also has effect on the back lobe suppression of the short tapered LWA. Figs. 10(a) and 10(b) show the simulated radiation pattern with different spacings for the CSRR structures at ground plane and on antenna plane, respectively. From the results, the back lobe obtains effective suppression while the spacing is about 0.4 mm.

Finally, the distance between the open-end edge of the LWA and the CSRR structure, $L_p$, has significant effect on back lobe suppression. Figs. 11 and 12 show the simulated radiation pattern results

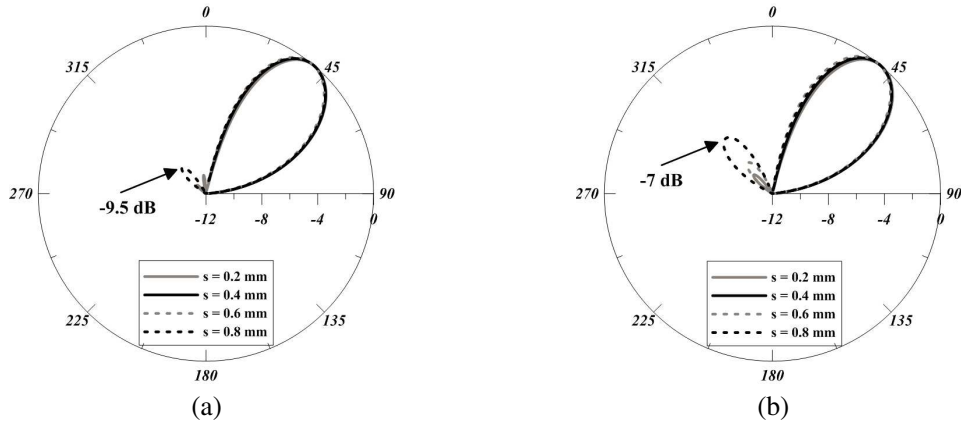


**Figure 10.** Simulated radiation patterns at 4.9 GHz with different spacing, $s$, where the perimeter $L_r$ is fixed to be 14.7 mm, the gap $g$ is fixed to be 1 mm and CSRR width $d$ is fixed to be 1 mm. (a) CSRR at ground plane. (b) CSRR on antenna plane.

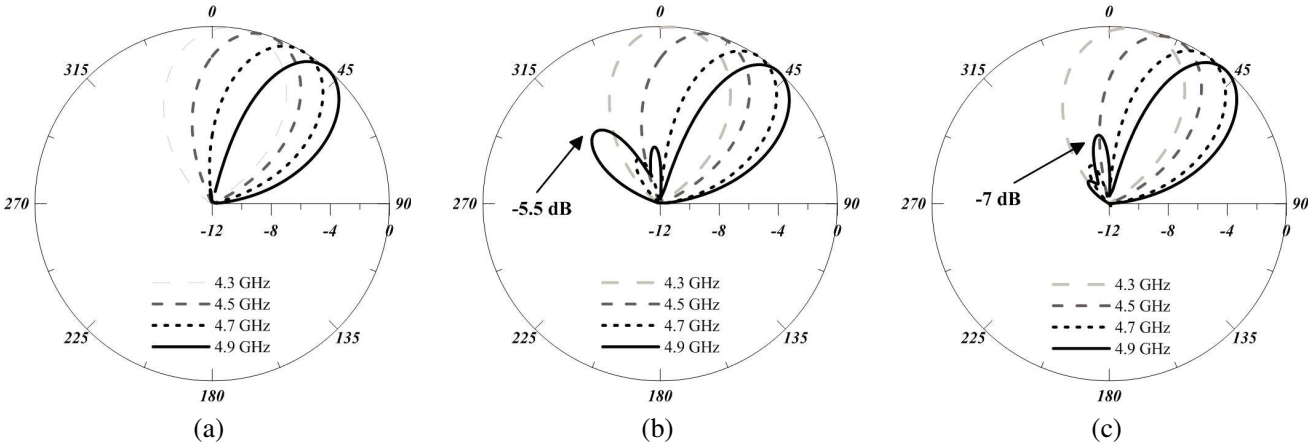


**Figure 11.** Radiation pattern simulation results with different distance, $L_p$, which is the distance between the CSRR structure and open-end of LWA for CSRR at ground plane. (a) $L_p = 7$ mm $(1/4\lambda_0)$. (b) $L_p = 14$ mm $(1/2\ \lambda_0)$. (c) $L_p = 21$ mm $(3/4\lambda_0)$.

with different $L_p$. According to the results, the back lobe can be suppressed effectively while the distance $L_p$ is chosen to be 7 mm which is about $1/4\lambda_g$ of 4.7 GHz away from the open-end edge of the LWA. The reason is described as following. The input wave feeds at input port of the LWA and propagates on the LWA. When the propagating wave delivers to the CSRR structure, some of them reflect back and some continues to propagate to the open-end edge of the LWA. Once the remaining wave propagates to the open-end edge, it also generates reflection at the edge. Both of these reflected waves will cause the back lobe since these waves are the backward waves. However, these two reflected waves can counteract each other while the CSRR structure is at a suitable position. When the distance between the CSRR structure and the open-end edge of the LWA is chosen to be about $1/4\lambda_g$, the back lobe of higher frequency band can be suppressed effectively. Since the reflected wave caused by the open-end edge of the LWA propagates about $1/2\lambda_g$ longer path, the phase difference between this wave and the reflected wave caused by the CSRR structure is about 180°. Therefore, the two reflected waves cancel each other, and the back lobe can be suppressed. Compared with other distance conditions, the back lobe is unable to be suppressed effectively, as displayed in Fig. 11.

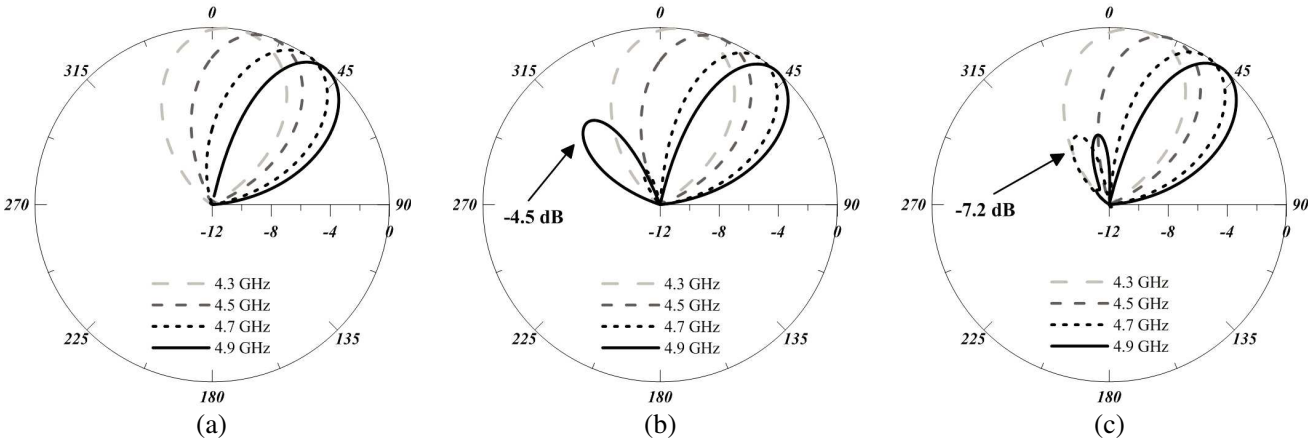


**Figure 12.** Radiation pattern simulation results with different distance, $L_p$, which is the distance between the CSRR structure and open-end of LWA for CSRR on antenna plane. (a) $L_p = 7\,\text{mm}$ $(1/4\lambda_0)$. (b) $L_p = 14\,\text{mm}$ $(1/2\lambda_0)$. (c) $L_p = 21\,\text{mm}$ $(3/4\lambda_0)$.

## 3. RESULTS

In this section, the measurement results of the short tapered LWA with CSRR structure are demonstrated. The two proposed antennas are fabricated as shown in Fig. 13 and Fig. 14. The return loss results are measured by Vector Network Analyzer (Agilent 5230A), and the radiation pattern results are obtained by an anechoic chamber as shown in Fig. 15.

The simulation and measurement normalized radiation pattern results are shown in Fig. 16 and Fig. 17 for the CSRR structures at ground plane and on antenna plane, respectively. These figures show the pattern when the antenna is operating at 4.3 GHz, 4.5 GHz, 4.7 GHz and 4.9 GHz. The measured radiation pattern results highly agree with the simulation ones. Meanwhile, the measurement results show that the back lobe has been suppressed better than 12 dB for the whole operating frequency band. It is shown that the CSRR structure can improve the back lobe level effectively. The comparison between simulation and measurement of maximum gain and return loss is illustrated in Fig. 18. There

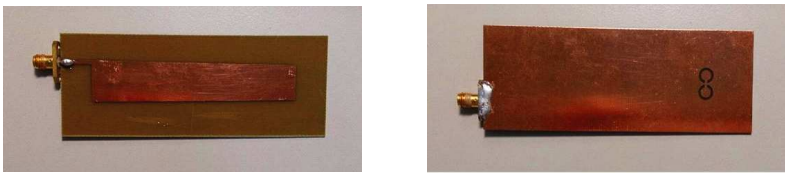


**Figure 13.** The fabricated proposed antenna with the CSRR structure at ground plane. (a) Top layer. (b) Bottom layer.

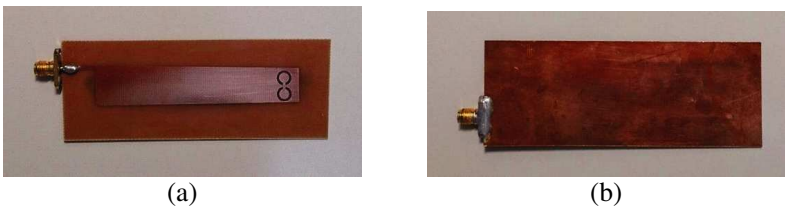


**Figure 14.** The fabricated proposed antenna with the CSRR structure on antenna plane. (a) Top layer. (b) Bottom layer.

**Figure 15.** The measurement setup in anechoic chamber.

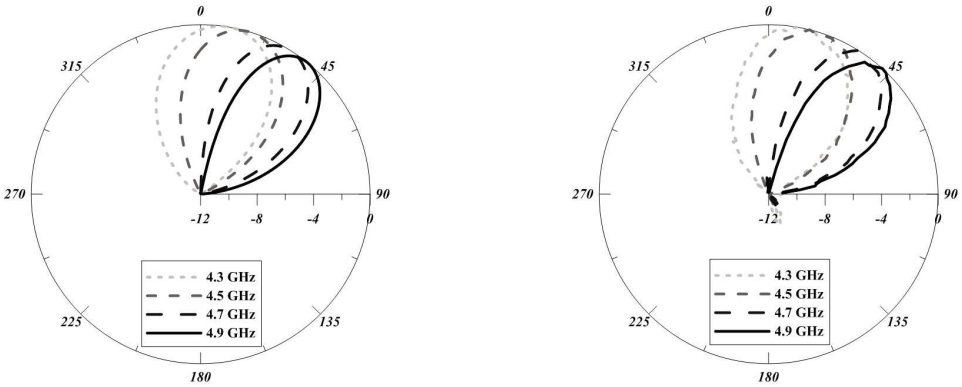


**Figure 16.** Simulation and measurement radiation pattern of proposed short tapered LWA with CSRR structure at ground plane. (a) Simulation. (b) Measurement.

is good agreement between the simulated and measured results. The average measured antenna gains is about 5.4 dBi and 5.34 dBi for the CSRR structures at ground plane and on antenna plane, respectively. Meanwhile, the measured impedance bandwidth of these two proposed short tapered LWA designs for 7-dB return loss is from 4.3 GHz to 4.95 GHz. Table 3 shows the back lobe level comparison results. The results indicate that the back lobe level has been improved better than 12 dB for the short (only $1.2\lambda_0$) tapered LWA by utilizing the CSRR structure. Both of the proposed short tapered LWAs have high back lobe suppression even operating at higher operating frequency.

**Table 3.** Back lobe level comparison (dB).

| Operating Frequency | Simulated of conventional LWA | Measured of tapered LWA | Measured of LWA with CSRR at ground plane | Measured of LWA with CSRR on antenna plane |
|---|---|---|---|---|
| 4.3 GHz | 7 | $> 30$ | $> 30$ | $> 30$ |
| 4.5 GHz | 5 | 17 | 23 | 22 |
| 4.7 GHz | 2 | 10 | 14 | 15 |
| 4.9 GHz | 1 | 8 | 13 | 13 |

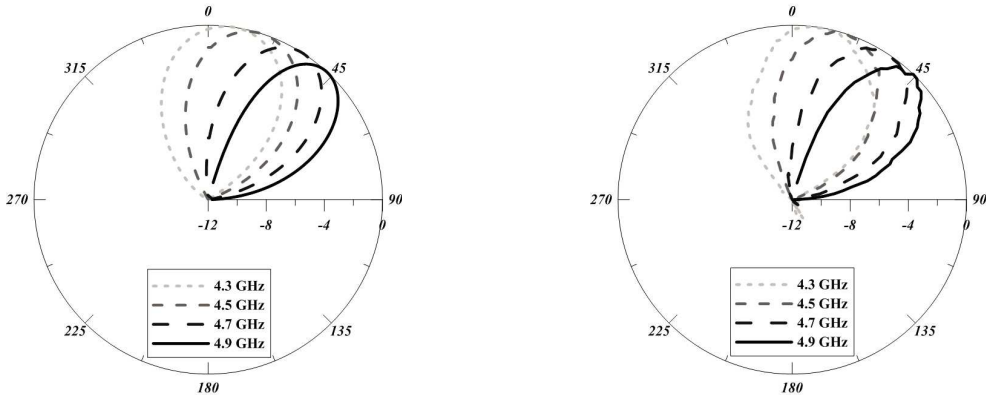


**Figure 17.** Simulation and measurement radiation pattern of proposed short tapered LWA with CSRR structure on antenna plane. (a) Simulation. (b) Measurement.

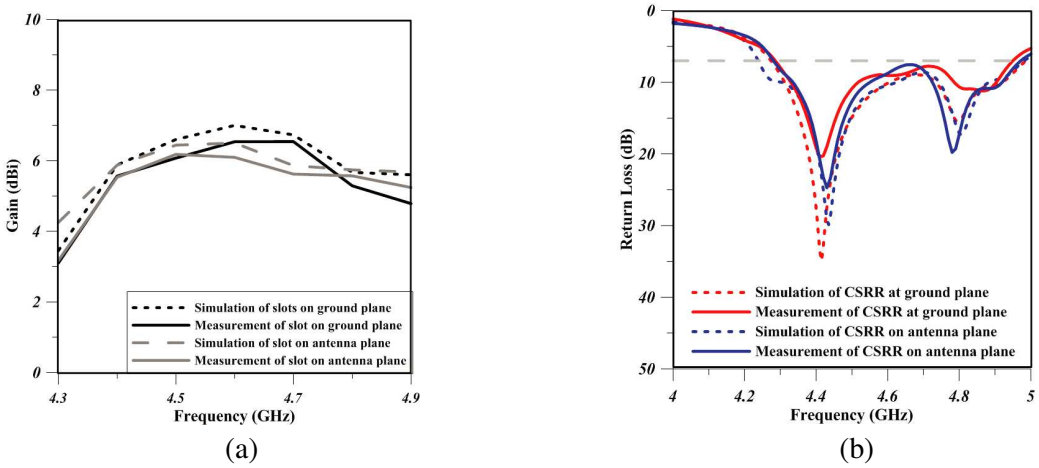


**Figure 18.** Comparison results between simulation and measurement. (a) Maxiumu gain. (b) Return loss.

## 4. CONCLUSION

In this paper, two novel short tapered LWAs with CSRR structure are proposed. The CSRR structure provides influence on the current distribution of the LWA. Firstly, the dimension of CSRR structure is related to the ability of the back lobe suppression. Secondly, the position of the CSRR structure is also a significant factor for suppressing back lobe. According to the measurement results, the 7-dB impedance bandwidth can be covered from 4.3 GHz to 4.95 GHz with the CSRR structure for both of the proposed antenna. The average measured antenna gains are about 5.4 dBi and 5.34 dBi for the CSRR structure on ground plane and antenna plane designs, respectively. The scanning angle of the measured main beam is about 34°, which covers the range from 10° to 44°. Furthermore, this proposed short tapered LWA structure with length only about $1.2\lambda_0$ at 4.3 GHz successfully suppresses the back lobe level better than 30 dB for operating frequency of 4.3 GHz and 13 dB for operating frequency of 4.9 GHz. For the whole operating frequency band, the back lobe level has been improved better than 12 dB for a short tapered LWA by the CSRR structure. To the authors' knowledge, this is the first publication using CSRR structure embedded to LWA design to improve back lobe suppression.

## ACKNOWLEDGMENT

The authors are grateful to the National Center for High performance Computing and the Chip Implementation Center (CIC) of National Applied Research Laboratories, Taiwan, for support with regard to simulation software and facilities. Meanwhile, this work was supported in part by the National Science Council (NSC), R.O.C., under contract NSC 102-2221-E-009 -028.

## REFERENCES

1. Menzel, W., "A new travelling wave antenna in microstrip," *8th European Microwave Conference*, 302–306, 1978.
2. Oliner, A. A. and K. S. Lee, "The nature of the leakage from higher modes on microstrip line," *IEEE Symposium on MTT-S International Digest*, 57–60, Baltimore, MD, USA, Jun. 1986.
3. Luxey, C. and J. M. Latheurte, "Simple design of dual-beam leaky-wave antennas in microstrips," *IEE Proceedings Microwaves, Antennas and Propagation*, Vol. 144, No. 6, 397–402, 1997.
4. Shih, Y., S. Chen, C. Hu, and C. F. Jou, "Active feedback microstrip leaky wave antenna-synthesiser design with suppressed back lobe radiation," *Electon. Lett.*, Vol. 35, No. 7, 513–514, 1999.
5. Guan, H., C. Wang, and C. F. Jou, "Suppression of reflected wave of leaky-wave antenna by utilizing an aperture-fed patch antenna," *Asia-Pacific Microwave Conference, APMC*, 966–969, Taipei, Taiwan, Dec. 2001.
6. Wang, C., H. Guan, and C. F. Jou, "A novel method for short leaky-wave antennas to suppress the reflected wave," *Microwave and Optical Tech. Lett.*, Vol. 36, No. 2, 129–131, 2003.
7. Chiou, Y., J. Wu, J. Huang, and C. F. Jou, "A novel short leaky-wave antenna for suppressing the back lobes," *International Workshop on Antenna Technology (iWAT)*, 1–4, Santa Monica, CA, USA, Feb. 2009.
8. Wu, J., C. Wang, and C. F. Jou, "Method of suppressing the side lobe of a tapered short leaky wave antenna," *IEEE Antennas and Wireless Propagat. Lett.*, Vol. 8, 1146–1149, 2009.
9. Wu, J., C. F. Jou, and C. Wang, "A compact wideband leaky-wave antenna with etched slot elements and tapered structure," *IEEE Trans. on Antennas and Propagat.*, Vol. 58, No. 7, 2176–2183, 2010.
10. Losito, O., M. Gallo, V. Dimiccoli, D. Barletta, and M. Bozzetti, "A tapered design of a CRLH-TL leaky wave antenna," *Proceedings of the 5th European Conference on Antennas and Propagation (EUCAP)*, 357–360, Rome, Apr. 2011.
11. Falcone, F., T. Lopetegi, J. D. Baena, R. Marqués, F. Martín, and M. Sorolla, "Effective negative-$\epsilon$ stopband microstrip lines based on complementary split ring resonators," *IEEE Microwave Wireless Compon. Lett.*, Vol. 14, No. 6, 280–282, 2004.
12. Pendry, J., B., A. J. Holden, D. J. Robbins, and W. J. Stewart, "Magnetism from conductors and enhanced nonlinear phenomena," *IEEE Trans. on Microwave Theory Tech.*, Vol. 47, No. 11, 2075–2084, 1999.
13. Niu, J. and X. Zhou, "Analysis of balanced composite right/left handed structure based on different dimensions of complementary split ring resonators," *Progress In Electromagnetics Research*, Vol. 74, 341–351, 2007.
14. Zhang, X., Z. Yu, and J. Xu, "Novel band-pass substrate integrated waveguide (SIW) filter based on complementary split ring resonators (CSRRs)," *Progress In Electromagnetics Research*, Vol. 72, 39–46, 2007.
15. Bahrami, H., M. Hakkak, and A. Pirhadi, "Analysis and design of highly compact bandpass waveguide filter using complementary split ring resonators (CSRR)," *Progress In Electromagnetics Research*, Vol. 80, 107–122, 2008.
16. Wu, G., W. Mu, X. Dai, and Y. Jiao, "Design of novel dual-band bandpass filter with microstrip meander-loop resonator and CSRR DGS," *Progress In Electromagnetics Research*, Vol. 78, 17–24, 2008.

17. Zhang, J., B. Cui, S. Lin, and X. Sun, "Sharp-rejection low-pass filter with controllable transmission zero using complementary split ring resonators (CSRRs)," *Progress In Electromagnetics Research*, Vol. 69, 219–226, 2007.
18. Ding, J., Z. Lin, Z. Ying, and S. He, "A compact ultra-wideband slot antenna with multiple notch frequency bands," *Microwave and Optical Tech. Lett.*, Vol. 49, No. 12, 3056–3060, 2007.
19. Braaten, B. D., "A novel compact UHF RFID tag antenna designed with series connected open complementary split ring resonator (OCSRR) particles," *IEEE Trans. on Antennas and Propagat.*, Vol. 58, No. 11, 3728–3733, 2010.
20. Anderson, J., K. Johnson, C. Satterlee, A. Lynch, and B. D. Braaten, "A reduced frequency printed quasi-Yagi antenna symmetrically loaded with meander open complementary split ring resonator (MOCSRR) elements," *IEEE International Symposium on Antennas and Propagation*, 270–273, Spokane, WA, USA, Jul. 2011.
21. Yuandan, D., H. Toyao, and T. Itoh, "Design and characterization of miniaturized patch antennas loaded with complementary split-ring resonators," *IEEE Trans. on Antennas and Propagat.*, Vol. 60, No. 2, 772–785, 2012.
22. Chang, D. C. and E. F. Kuester, "Total and partial reflection from the end of a parallel-plate waveguide with an extended dielectric slab," *Radio Science*, Vol. 16, No. 1, 1–13, 1981.
23. Oliner, A. A. and K. S. Lee, "Microstrip leaky wave strip antennas," *IEEE Symposium on Antennas and Propagation*, Vol. 24, 443–446, Philadelphia, PA, USA, Jun. 1986.
24. Caloz, C. and T. Itoh, *Electromagnetic Metamaterials: Transmission Line Theory and Microwave Applications*, Wiley-IEEE Press, 2005.